



Title	Cibacron blue 3G-A is a novel inhibitor of Otopetrin 1 (OTOP1), a proton channel
Author(s)	Islam, MD Mominul; Sasaki, Omi; Yano-Nashimoto, Saori; Okamatsu-Ogura, Yuko; Yamaguchi, Soichiro
Citation	Biochemical and biophysical research communications, 665, 64-70 https://doi.org/10.1016/j.bbrc.2023.04.112
Issue Date	2023-04-29
Doc URL	http://hdl.handle.net/2115/92064
Rights	© 2023. This manuscript version is made available under the CC-BY-NC-ND 4.0 license http://creativecommons.org/licenses/by-nc-nd/4.0/
Rights(URL)	https://creativecommons.org/licenses/by-nc-nd/4.0/
Type	article (author version)
File Information	SYamaguchi For HUSCAP.pdf



[Instructions for use](#)

Cibacron Blue 3G-A is a novel inhibitor of Otopetrin 1 (OTOP1),
a proton channel

MD Mominul Islam¹, Omi Sasaki¹, Saori Yano-Nashimoto¹,

Yuko Okamatsu-Ogura², and Soichiro Yamaguchi¹

¹ Laboratory of Physiology, Department of Basic Veterinary Sciences, Faculty of Veterinary

Medicine, Hokkaido University, Sapporo, Hokkaido, 060-0818, Japan

² Laboratory of Biochemistry, Department of Basic Veterinary Sciences, Faculty of Veterinary

Medicine, Hokkaido University, Sapporo, Hokkaido, 060-0818, Japan

Correspondence:

Soichiro Yamaguchi, Laboratory of Physiology, Department of Basic Veterinary Sciences, Faculty of

Veterinary Medicine, Hokkaido University, Sapporo, Hokkaido, 060-0818, Japan

Tel.: +81-11-706-5200

Fax: +81-11-706-5202

E-mail address: souya@vetmed.hokudai.ac.jp

¹

¹ **Abbreviations:**

cDNA, complementary DNA; CsOH, cesium hydroxide; DMSO, dimethyl sulfoxide; EGFP, enhanced green fluorescence protein; EGTA, ethylene glycol tetraacetic acid; HEPES, 4-(2-hydroxyethyl)piperazine-1-ethanesulfonic acid; MES, 2-morpholinoethanesulphonic acid; *mOtop1*, mouse *Otop 1*; NMDG, N-methyl-D-glucamine; OTOP1, Otopetrin 1

Abstract

Otopetrin 1 (OTOP1) is a proton (H^+) channel which detects acidic stimuli in sour taste receptor cells and plays some sort of role in the formation of otoconia in the inner ear.

Although it is known that zinc ion (Zn^{2+}) inhibits OTOP1, Zn^{2+} requires high concentrations (mM order) to inhibit OTOP1 sufficiently, and no other inhibitors have been found.

Therefore, to identify a novel inhibitor, we screened a chemical library (LOPAC¹²⁸⁰) by whole-cell patch clamp recordings, measuring proton currents of heterologously-expressed mouse OTOP1. From the screening, we found that reactive blue 2 inhibited OTOP1 currents.

Further evaluations of three analogues of reactive blue 2 revealed that cibacron blue 3G-A potently inhibited OTOP1 currents. Cibacron blue 3G-A inhibited OTOP1 currents in a

concentration-dependent manner, and its 50% inhibitory concentration (IC₅₀) and the Hill coefficient were 5.0 μ M and 1.1, respectively. The inhibition of OTOP1 currents by cibacron

blue 3G-A was less affected by extracellular anion compositions, membrane potentials, and low pH than the inhibition by Zn^{2+} . These results suggest that the inhibition of OTOP1 by cibacron

blue 3G-A is neither likely to be a pore-blocking inhibition nor a competitive inhibition.

Furthermore, our findings revealed that cibacron blue 3G-A can be used as a novel inhibitor of

OTOP1 especially under the conditions in which OTOP1 activity is evaluated such as low pH.

Keywords:

Otopetrin1, OTOPI, proton channel, reactive blue 2, cibacron blue 3G-A

1. Introduction

Otopetrin 1 (OTOPI) was at first discovered as a multi-transmembrane protein, mutations of which impeded the development of otoconia (or otolith) in the vestibular system [1,2]. Later, OTOPI was revealed to be a proton (H^+) channel which detects acidic stimuli in sour taste receptors [3].

Since the functional role of OTOPI in the otoconia formation has not been revealed [1], inhibitors of OTOPI will be a useful tool for clarifying the role of OTOPI. However, no inhibitor of OTOPI has been reported yet except for the Zn^{2+} [3–5]. Although Zn^{2+} inhibits the proton currents of OTOPI, Zn^{2+} requires high concentrations (mM order) to inhibit OTOPI sufficiently, and the inhibition is weakened by lowering the extracellular pH [3–6]. Zn^{2+} also inhibits numerous ion channels, such as voltage-dependent Ca^{2+} channels, voltage-gated Na^+ channels, several potassium channels, ligand (NMDA, GABA)-gated channels, TRP channels, and others [7,8]. Moreover, Zn^{2+} is an essential trace element, which has a large number of physiological roles, and contrarily has a toxic effect if excess is infused [9]. Therefore, Zn^{2+} cannot be stated as a good inhibitor of OTOPI and is not appropriate for *in vivo* administration.

Therefore, in this study, in order to identify a novel OTOPI inhibitor, we screened 1280 compounds in a chemical library, LOPAC¹²⁸⁰ (Merck, Darmstadt, Germany) using a heterologous

expression system (mouse OTOPI expressed in CHO-K1 cells) and whole-cell patch clamp recordings. From the library, we identified reactive blue 2 as a novel inhibitor of OTOPI. Further evaluations of reactive blue 2 analogues revealed that cibacron blue 3G-A potently inhibited OTOPI currents. We also analyzed the inhibitory features of OTOPI currents by cibacron blue 3G-A while comparing them with those by Zn^{2+} and found that there are some advantages in cibacron blue 3G-A as an inhibitor of OTOPI.

2. Materials and Methods

2.1 Plasmid constructions and cell transfection

A full-length mouse *Otop1* (*mOtop1*) complementary DNA (cDNA) was amplified by PCR from mouse (C57BL/6J, male) brown adipose tissue cDNA, which was produced in the previous research [10]. The *mOtop1* cDNA was cloned into a pmCherry-C1 (Takara Bio, Otsu, Shiga, Japan) vector or a pIRES2-EGFP (Clontech, Mountain View, CA, USA) vector. The encoded amino acid sequence of mOTOPI was almost identical to the sequence deposited in GenBank (GenBank accession #NP_766297.2) except for 396th alanine, which is glycine in NP_766297.2. The *mOtop1*-pmCherry-C1 was used for the screening of LOPAC¹²⁸⁰, and other experiments were conducted using the *mOtop1*-pIRES2-EGFP. The vectors were transiently transfected into CHO-K1 (RIKEN BRC, Tsukuba, Ibaraki, Japan) cells using Trans-IT 293 transfection reagent (Takara Bio). Membrane

currents were recorded from mCherry- or enhanced green fluorescence protein (EGFP)-positive single cells on the next day after the transfection. Empty vector (pmCherry-C1 or pIRES2-EGFP) transfected cells did not show inward currents by perfusion of acidic solutions (the differences between the current amplitudes at -100 mV under pH 5.0, 5.5, and 6.0 and those under pH 7.4 were between -0.9 and 6.8 pA ($n = 3$)).

2.2 Whole-cell patch-clamp experiments

The methods used for measurements and analysis of whole-cell currents were similar to those reported previously [11]. The membrane potential was held at 0 mV and varied from -100 to $+100$ mV (with ramp pulse) over a duration of 400 msec following a prepulse of -100 mV for 50 msec every 5 sec. To minimize pH alteration, the pipette solution contained a high concentration (200 mM) of a pH buffer, 4-(2-hydroxyethyl)piperazine-1-ethanesulfonic acid (HEPES) (pH 7.3 with cesium hydroxide (CsOH)). Bath solutions for the measurements of OTOP1 currents were N-methyl-D-glucamine (NMDG)-glutamate or NMDG-Cl rich HEPES- or 2-morpholinoethanesulphonic acid (MES)-buffered solutions (pH 5.0 - 7.4). The detailed compositions of solutions are listed in Table 1. The liquid junction potentials were not corrected. Currents were low-pass filtered at 1 kHz and sampled at 5 kHz. All experiments were performed at room temperature.

The screening of LOPAC¹²⁸⁰ was conducted by evaluating inhibitory effects of mixtures of five

compounds (each concentration was 0.5 μ M) on OTOPI currents under the pH 5.5 solution. When a mixture inhibited more than 10% of the OTOPI current amplitude (a current amplitude under pH 5.5 – that under pH 7.4) at -100 mV, each compound of the mixture was re-evaluated separately. To eliminate the effect of the solvent (dimethyl sulfoxide (DMSO)), the control pH 5.5 solution without compounds also contained the same amount of DMSO when LOPAC¹²⁸⁰ and reactive blue 2 analogues were screened. In other experiments, the control solutions did not contain DMSO, but it was confirmed that DMSO did not inhibit OTOPI currents (the remaining current percentage was $98.6 \pm 1.2\%$ under the NMDG-glutamate-rich pH 5.5 solution (n = 4)).

2.3 Data analyses

The 50% inhibitory concentration (IC50) of inhibitors was computed using KyPlot 6.0 (KYENSLAB INC., Chiyoda-ku, Tokyo, Japan) by fitting the concentration–response curve with the Hill equation:

$$f(x) = 100/(1 + (x/IC50)^{nH})$$

where x is the concentration of an inhibitor, and nH is the Hill coefficient.

All average results are presented as means \pm S.E. of independent experiments (n). Two-tailed unpaired Student's t-test, One-way ANOVA, and Dunnett's test were used to determine P values. Statistical significance was defined as $P < 0.05$.

2.4 Drugs

LOPAC¹²⁸⁰ (Merck, Darmstadt, Germany), each compound of which was diluted to 1 mM with DMSO, was provided by Center for Supporting Drug Discovery and Life Science Research, Graduate School of Pharmaceutical Science, Osaka University under the support of BINDS (Basis for Supporting Innovative Drug Discovery and Life Science Research) and stored at -30°C . Reactive blue 2 (synonym: procion blue HB) was obtained from BLD pharmatech (Shanghai, China). Remazol brilliant blue R salt was obtained from nacalai tesque (Kyoto, Japan). Reactive blue 4 and cibacron blue 3G-A were obtained from MedChemExpress (Monmouth Junction, NJ, USA). Stock solutions of these compounds were dissolved in DMSO at a concentration of 100 mM and stored at -30°C .

3. Results

3.1 Reactive blue 2 inhibits OTOP1

In the first screening, the mixture of five compounds including reactive blue 2 inhibited 19.6% of OTOP1 currents. In the re-evaluation of the five compounds, reactive blue 2 (0.5 μM ; its chemical structure is shown in Fig. 1A) showed the highest inhibition (8.5%) of OTOP1 currents among the five compounds. Therefore, we bought reactive blue 2 and examined its effect in a higher concentration (100 μM). One hundred μM reactive blue 2 inhibited about 50% of OTOP1 currents under pH 5.5 and

its inhibition was reversible (Figs. 1B and 1C). This result indicates that reactive blue 2 is a novel inhibitor of OTOPI. However, the 50% inhibition by 100 μ M implies that the inhibitor is not potent. Therefore, we examined analogues of reactive blue 2.

3.2 Cibacron blue 3G-A potently inhibits OTOPI

The reactive blue 2 analogues which we examined were reactive blue 4, remazol brilliant blue R salt, and cibacron blue 3G-A (Fig. 2A). The all three analogues inhibited OTOPI currents but cibacron blue 3G-A showed the strongest inhibition of OTOPI currents (Figs. 2B and 2C). Cibacron blue 3G-A is an isomer of reactive blue 2 (Figs. 1A and 2A, the different group is underlined). OTOPI currents were inhibited by cibacron blue 3G-A in a concentration-dependent manner (Figs. 3A and 3B). The IC50 and Hill coefficient, which were obtained by fitting to the Hill equation, were 5.0 μ M and 1.1, respectively.

3.3 Cibacron blue 3G-A is less affected by extracellular anion compositions, membrane potentials, and pH than Zn²⁺

We analyzed the inhibitory features of OTOPI currents by cibacron blue 3G-A while comparing them with those by Zn²⁺.

Firstly, in the patch clamp measurements, organic anions such as glutamate, which was used in

this study, are often used to avoid contamination of chloride currents. However, we found that the inhibition of OTOPI currents by Zn^{2+} in the glutamate-rich solution was significantly weaker than that in the chloride-rich solution (Figs. 4A and 4B). We did not reveal the mechanism of the reduction in the potency of Zn^{2+} in the glutamate-rich solution, but this might be due to the chelation of Zn^{2+} by glutamate [12]. On the other hand, the inhibition by cibacron blue 3G-A showed no significant change whether the chloride-rich solution or the glutamate-rich solution was used (Figs. 4C and 4D. the IC50s and the Hill coefficients under the chloride-rich solution and under the glutamate-rich solution were 4.5 μ M and 1.1, and 5.0 μ M and 1.1, respectively).

Secondly, the inhibition of OTOPI currents by Zn^{2+} was affected by membrane potentials (Fig. 4E) although it has been reported that inhibition by Zn^{2+} was voltage independent [4,13]. On the other hand, the inhibition by cibacron blue 3G-A was not significantly different from -100 mV to -40 mV. The discrepancy in the voltage dependency of Zn^{2+} between our result and the literature might be due to the difference in the method of analysis. At least, however, the inhibition by cibacron blue 3G-A seems to be less voltage dependent than that of Zn^{2+} when they were compared by the same analysis.

Finally, the inhibition of OTOPI currents by Zn^{2+} (1 mM) was dependent on the extracellular pH (Fig. 4F) as reported elsewhere [4,5]. On the other hand, the inhibition by cibacron blue 3G-A (10 μ M) was not significantly different whether pH 5.0, 5.5, or 6.0 solutions were used (Fig. 4F). The IC50s and the Hill coefficients at pH 5.0, pH 5.5, and pH 6.0 were 3.4 μ M and 1.0, 5.0 μ M and 1.1, and 5.2

μM and 1.0, respectively (Fig. 4G).

Discussion

The inhibitory features which were observed in this study provided a few insights into the mechanism of the OTOPI inhibition by cibacron blue 3G-A. The inhibition of OTOPI by cibacron blue 3G-A is neither likely to be a competitive inhibition nor a pore-blocking inhibition because the inhibition was independent of pH (i.e. the concentration of H^+ , which is the ion conducted by OTOPI) (Figs. 4F and 4G) and membrane potentials (Fig. 4E), respectively. Hill coefficients obtained by fitting to the Hill equation were also around 1.0 (Figs. 3B, 4D and 4G). This suggests that there seems to be just one binding site of cibacron blue 3G-A in OTOPI, or if there are multiple sites, the bindings show no cooperativity [14]. Although the binding site of cibacron blue 3G-A in OTOPI was not revealed in this study, structural analyses using x-ray crystallography or Cryo-EM of cibacron 3G-A-bound OTOPI structure may identify it. Moreover, such analyses might be useful for understanding how OTOPI changes its conformation to conduct H^+ if the binding of cibacron blue 3G-A fixes a conformation of OTOPI.

Cibacron blue 3G-A has advantages as an OTOPI inhibitor comparing with Zn^{2+} . Firstly, cibacron blue 3G-A can inhibit OTOPI at lower concentrations than Zn^{2+} as the inhibition by 10 μM cibacron blue 3G-A was comparable with that by 1 mM Zn^{2+} (Fig. 4E). Secondly, cibacron blue 3G-A is less

affected by extracellular anion composition, membrane depolarizations, and low pH than Zn^{2+} (Fig. 4). When measuring proton currents, lower pH solutions are used. And in order to reduce contamination of chloride currents, glutamate-rich solutions can be used as mentioned above. When OTOPI conducts H^+ in an intact cell during cell physiological experiments, the membrane potential is likely to be depolarized as observed in sour taste receptor cells [4,6]. In such conditions, the inhibition of OTOPI by Zn^{2+} is assumed to become weaker, while cibacron blue 3G-A is supposed to be less affected (or might be more potent in acidic conditions as the IC50 was rather slightly lower at pH 5.0 than pH 6.0).

Although Zn^{2+} inhibits numerous ion channels other than OTOPI [7,8], cibacron blue 3G-A also inhibits other proteins. Cibacron blue 3G-A is known to block P2X and P2Y purinergic receptors (and simultaneously potentiate P2X₃ and P2X₄ receptors) at μM order concentrations [15–19]. When cibacron blue 3G-A is used for the inhibition of OTOPI, its blocking of P2 receptors should be taken into account, and vice versa. Cibacron blue 3G-A was also reported to inhibit cytosolic enzymes, such as lactate dehydrogenase and glutathione S transferase, and Na^+K^+ -ATPase by binding to the nucleotide binding site in the intracellular side [20–22]. As cibacron blue 3G-A contains charged sulfate groups, it seems to be membrane impermeable at physiological pH. However, reactive blue 2, the isomer of cibacron blue 3G-A, was reported to be taken up into the cytosol of rat C6 glioma cells after its incubation for hours [23]. Therefore, when analyses of cell functions require long-time

incubation with cibacron blue 3G-A, its side effects on cytosolic proteins also need to be considered even if it is applied extracellularly. Moreover, the effects of cibacron blue 3G-A on other proton channels (Hv channel, OTO2, and OTO3) have not been evaluated. If the specificity of cibacron blue 3G-A among the proton channels is revealed, the inhibition by cibacron blue 3G-A might be able to discriminate these proton channels.

With the cautions mentioned above, however, cibacron blue 3G-A can be used for the evaluations of alterations in cell functions when OTO1 function is inhibited. At least, the inhibition by cibacron blue 3G-A can be treated as one of the necessary conditions for the identification of OTO1 currents by patch clamp measurements in addition to the inhibition by Zn^{2+} .

Finally, based on the findings obtained in this study, better inhibitors of OTO1 might be able to be developed by using cibacron blue 3G-A as a lead compound. If more specific inhibitors are developed, they will be more useful for research on the physiological roles of OTO1. Furthermore, such specific inhibitors might be able to be used for the clinical treatment of dysgeusia (taste disorders, such as phantogeusia, and parageusia) which are associated with sour taste by inhibiting OTO1 although such dysgeusia is relatively less prevalent [23].

Declaration of competing interest

The authors declare no actual or potential competing interests.

Acknowledgements

This work was supported by Lotte Foundation (to S.Y.), JSPS KAKENHI Grant Number 22K06825 (to S.Y.), and a Grant-in-Aid for Graduate Student from the World-leading Innovative and Smart Education (WISE) Program (1801) from the Ministry of Education, Culture, Sports, Science, and Technology, Japan (to M.M.I.). This research was also partially supported by Platform Project for Supporting Drug Discovery and Life Science Research (Basis for Supporting Innovative Drug Discovery and Life Science Research (BINDS)) from AMED under Grant Number JP21am0101084 (support number 2806).

References

- [1] S. Huang, S. Qian, Advances in otolith-related protein research, *Front. Neurosci.* 16 (2022) 1–9. <https://doi.org/10.3389/fnins.2022.956200>.
- [2] I. Hughes, J. Binkley, B. Hurle, E.D. Green, R. Blakesley, G. Bouffard, J. McDowell, B. Maskeri, N. Hansen, M. Park, P. Thomas, A. Young, A. Sidow, D.M. Ornitz, Identification of the Otopetrin Domain, a conserved domain in vertebrate otopetrins and invertebrate otopetrin-like family members, *BMC Evol. Biol.* 8 (2008) 1–10. <https://doi.org/10.1186/1471-2148-8-41>.
- [3] Y.-H. Tu, A.J. Cooper, B. Teng, R.B. Chang, D.J. Artiga, H.N. Turner, E.M. Mulhall, W. Ye,

- A.D. Smith, E.R. Liman, An evolutionarily conserved gene family encodes proton-selective ion channels., *Science*. 359 (2018) 1047–1050. <https://doi.org/10.1126/science.aao3264>.
- [4] J.D. Bushman, W. Ye, E.R. Liman, A proton current associated with sour taste: Distribution and functional properties, *FASEB J.* 29 (2015) 3014–3026. <https://doi.org/10.1096/fj.14-265694>.
- [5] B. Teng, C.E. Wilson, Y.H. Tu, N.R. Joshi, S.C. Kinnamon, E.R. Liman, Cellular and Neural Responses to Sour Stimuli Require the Proton Channel Otop1, *Curr. Biol.* 29 (2019) 3647-3656.e5. <https://doi.org/10.1016/j.cub.2019.08.077>.
- [6] R.B. Chang, H. Waters, E.R. Liman, A proton current drives action potentials in genetically identified sour taste cells, *Proc. Natl. Acad. Sci. U. S. A.* 107 (2010) 22320–22325. <https://doi.org/10.1073/pnas.1013664107>.
- [7] A. Bouron, K. Kiselyov, J. Oberwinkler, Permeation, regulation and control of expression of TRP channels by trace metal ions, *Pflugers Arch. Eur. J. Physiol.* 467 (2015) 1143–1164. <https://doi.org/10.1007/s00424-014-1590-3>.
- [8] S. Noh, S.R. Lee, Y.J. Jeong, K.S. Ko, B.D. Rhee, N. Kim, J. Han, The direct modulatory activity of zinc toward ion channels, *Integr. Med. Res.* 4 (2015) 142–146. <https://doi.org/10.1016/j.imr.2015.07.004>.
- [9] C. Livingstone, Zinc: Physiology, deficiency, and parenteral nutrition, *Nutr. Clin. Pract.* 30 (2015) 371–382. <https://doi.org/10.1177/0884533615570376>.

- [10] Y. Okamatsu-Ogura, M. Kuroda, R. Tsutsumi, A. Tsubota, M. Saito, K. Kimura, H. Sakaue, UCP1-dependent and UCP1-independent metabolic changes induced by acute cold exposure in brown adipose tissue of mice, *Metabolism*. 113 (2020) 154396. <https://doi.org/10.1016/j.metabol.2020.154396>.
- [11] S. Yamaguchi, A. Tanimoto, K. Otsuguro, H. Hibino, Negatively Charged Amino Acids Near and in Transient Receptor Potential (TRP) Domain of TRPM4 Channel Are One Determinant of Its Ca^{2+} Sensitivity, (2014). <https://doi.org/10.1074/jbc.M114.606087>.
- [12] M. Spiridon, D. Kamm, B. Billups, P. Mobbs, D. Attwell, Modulation by zinc of the glutamate transporters in glial cells and cones isolated from the tiger salamander retina, *J. Physiol*. 506 (1998) 363–376. <https://doi.org/10.1111/j.1469-7793.1998.363bw.x>.
- [13] L. Tian, H. Zhang, S. Yang, A. Luo, P.M. Kamau, J. Hu, L. Luo, R. Lai, Vertebrate OTOPI1 is also an alkali-activated channel, *Nat. Commun*. 14 (2023). <https://doi.org/10.1038/s41467-022-35754-9>.
- [14] H. Prinz, Hill coefficients, dose-response curves and allosteric mechanisms., *J. Chem. Biol*. 3 (2010) 37–44. <https://doi.org/10.1007/s12154-009-0029-3>.
- [15] A.D. Michel, C.B.A. Grahames, P.P.A. Humphrey, Functional characterisation of P2 purinoceptors in PC12 cells by measurement of radiolabelled calcium influx, *Naunyn-Schmiedeberg's Arch. Pharmacol*. 354 (1996) 562–571. <https://doi.org/10.1007/BF00170829>.

- [16] K. Alexander, W. Niforatos, B. Bianchi, E.C. Burgard, K.J. Lynch, E.A. Kowaluk, M.F. Jarvis, T. Van Biesen, Allosteric modulation and accelerated resensitization of human P2X3 receptors by cibacron blue, *J. Pharmacol. Exp. Ther.* 291 (1999) 1135–1142.
- [17] J. Brown, C.A. Brown, Evaluation of reactive blue 2 derivatives as selective antagonists for P2Y receptors, *Vascul. Pharmacol.* 39 (2002) 309–315. [https://doi.org/10.1016/S1537-1891\(03\)00030-2](https://doi.org/10.1016/S1537-1891(03)00030-2).
- [18] F. Tuluc, R. Bültmann, M. Glänzel, A.W. Frahm, K. Starke, P2-receptor antagonists: IV. Blockade of P2-receptor subtypes and ecto-nucleotidases by compounds related to reactive blue 2, *Naunyn. Schmiedebergs. Arch. Pharmacol.* 357 (1998) 111–120. <https://doi.org/10.1007/PL00005144>.
- [19] K.J. Miller, A.D. Michel, I.P. Chessell, P.P.A. Humphrey, Cibacron blue allosterically modulates the rat P2X4 receptor, *Neuropharmacology.* 37 (1998) 1579–1586. [https://doi.org/10.1016/S0028-3908\(98\)00153-1](https://doi.org/10.1016/S0028-3908(98)00153-1).
- [20] M. Kalim Tahir, C. Guthenberg, B. Mannervik, Inhibitors for distinction of three types of human glutathione transferase, *FEBS Lett.* 181 (1985) 249–252. [https://doi.org/10.1016/0014-5793\(85\)80269-6](https://doi.org/10.1016/0014-5793(85)80269-6).
- [21] V. Durisová, A. Vrbanová, A. Ziegelhoffer, A. Breier, Interaction of Cibacron Blue 3GA and Remazol Brilliant Blue R with the nucleotide binding site of lactate dehydrogenase and (Na⁺ +

- K⁺)-ATPase., *Gen. Physiol. Biophys.* 9 (1990) 519–528.
- [22] A. Breier, V. Boháčová, P. Dočolomanský, Inhibition of (Na⁺/K⁺)-ATPase by Cibacron blue 3G-A and its analogues, *Gen. Physiol. Biophys.* 25 (2006) 439–453.
- [23] P. Claes, K. Van Kolen, D. Roymans, D. Blero, K. Vissenberg, C. Erneux, J.P. Verbelen, E.L. Esmans, H. Slegers, Reactive blue 2 inhibition of cyclic AMP-dependent differentiation of rat C6 glioma cells by purinergic receptor-independent inactivation of phosphatidylinositol 3-kinase, *Biochem. Pharmacol.* 67 (2004) 1489–1498. <https://doi.org/10.1016/j.bcp.2003.12.017>.

Figure legends

Fig. 1. Reactive blue 2 was found as an inhibitor of OTOPI by screening LOPAC¹²⁸⁰.

(A) Chemical structures of reactive blue 2. Reactive blue 2 is a mixture of two isomers with a distinct sulphonic acid, which is underlined with a dashed red line, in meta (left) or para (right) position [18].

(B) Representative I-V curves of whole-cell currents. One hundred micro molar reactive blue 2, which was dissolved in a pH 5.5 solution, was applied extracellularly (Reactive Blue 2; red line). Before (before; blue line) and after (wash; green line) the application of reactive blue 2, a pH 5.5 solution with the solvent (0.1% DMSO) was perfused. To subtract leak currents, a pH 7.4 solution was also perfused (pH 7.4; black line). (C) A summary of remaining current amplitudes in the presence of 100

μM reactive blue 2 (Reactive Blue 2; red bar), which were normalized to the current amplitude before its application (before; blue bar). After washing, current amplitudes were recovered (wash; green bar). To avoid influence of rundown of current amplitudes, data were collected only when the current amplitudes recovered more than 90% of initial values after washing (the same criterion was applied to all following experiments). Shown are means \pm S.E. ($n = 5$), (** $p < 0.01$ vs. before, Dunnett's test).

Fig. 2. Cibacron blue 3G-A was the most potent inhibitor among reactive blue 2 analogues examined.

(A) Chemical structures of reactive blue 2 analogues examined (from left to right, Reactive Blue 4, Remazol Brilliant Blue R salt, and Cibacron Blue 3G-A). Cibacron blue 3G-A is an isomer of reactive blue 2 with a distinct sulphonic acid, which is underlined with a dashed red line, in ortho position. (B) Representative I-V curves of whole-cell currents. One hundred micro molar reactive blue 2 analogues (Reactive Blue 4, Remazol Brilliant Blue R, and Cibacron Blue 3G-A), which were dissolved in a pH 5.5 solution, were applied extracellularly (red line). Before (blue line) and after (wash; green line) the application of the reactive blue 2 analogues, a pH 5.5 solution with the solvent (0.1% DMSO) was perfused. To subtract leak currents, a pH 7.4 solution was also perfused (pH 7.4; black line). (C) Summaries of remaining current amplitudes in the presence of 100 μM reactive blue 2 analogues (Reactive Blue 4, Remazol Brilliant Blue R, and Cibacron Blue 3G-A; red bar), which were

normalized to the current amplitude before its application (before; blue bar). Green bars show the normalized current amplitudes after washing (wash). Shown are means \pm S.E. (n = 4 to 7. *p < 0.05, **p < 0.01 vs. before, Dunnett's test).

Fig. 3. Concentration-inhibitory curve of cibacron blue 3G-A

(A) Representative I-V curves of whole-cell currents. Different concentrations (1-100 μ M) of cibacron blue 3G-A, which were dissolved in an NMDG-glutamate-rich pH 5.5 solution, were applied extracellularly (red line). Before (blue line) and after (wash; green line) the application of cibacron blue 3G-A, the pH 5.5 solution was perfused. To subtract leak currents, a pH 7.4 solution was also perfused (pH 7.4; black line). (B) The horizontal axis indicates cibacron blue 3G-A concentrations (μ M). The vertical axis indicates percentage of remaining OTOPI current amplitudes, which were normalized to that before application, at -100 mV in the presence of cibacron blue 3G-A (1-100 μ M). Shown are mean \pm S.E. (n = 4 or 5). The line was drawn by fitting to the Hill equation.

Fig. 4. Comparison of inhibitory features of Zn^{2+} and those of cibacron blue 3G-A

(A) Representative I-V curves of whole-cell currents. One mM Zn^{2+} , which was dissolved in the chloride-rich pH 5.5 solution (left) or in the glutamate-rich pH 5.5 solution (right), was applied extracellularly (red line). Before (blue line) and after (wash; green line) the application of Zn^{2+} , the

pH 5.5 solution was perfused. To subtract leak currents, a pH 7.4 solution was also perfused (pH 7.4; black lines). (B) Percent inhibitions of OTOPI currents by 1 mM Zn^{2+} at -100 mV in the chloride-rich pH 5.5 solution (white bar) or in the glutamate-rich pH 5.5 solution (black bar). Shown are mean \pm S.E. ($n = 4$ or 5 . $**p < 0.01$, Student's t-test). (C) Percent inhibitions of OTOPI currents by 10 μ M cibacron blue 3G-A at -100 mV in the chloride-rich pH 5.5 solution (white bar) or in the glutamate-rich pH 5.5 solution (black bar). Shown are mean \pm S.E. ($n = 4$ or 5 . N.S.: not significant, Student's t-test). (D) Concentration-inhibitory curves of cibacron blue 3G-A in the chloride-rich pH 5.5 solution (white square) or in the glutamate-rich pH 5.5 solution (black circle, the same data with Fig. 3B). Shown are mean \pm S.E. ($n = 4$ or 5). Error bars smaller than symbols are not shown (the same applies hereinafter). The lines were drawn by fitting to the Hill equation (glutamate: solid line, chloride: dotted line). (E) Percent inhibitions of OTOPI currents by 10 μ M cibacron blue 3G-A (blue circle) or by 1 mM Zn^{2+} (orange triangle) at -100 mV, -80 mV, -60 mV, and -40 mV. Shown are mean \pm S.E. ($n = 4$. $**p < 0.01$, N.S.: not significant, One-way ANOVA). (F) Percent inhibitions of OTOPI currents by 10 μ M cibacron blue 3G-A (blue circle) or by 1 mM Zn^{2+} (orange triangle) in the glutamate-rich pH 5.0, 5.5, or 6.0 solutions at -100 mV. Shown are mean \pm S.E. ($n = 4$ or 5 , $**p < 0.01$, N.S.: not significant, One-way ANOVA). (G) Concentration-inhibitory curves of cibacron blue 3G-A in the chloride-rich pH 5.0 (red triangle), 5.5 (black circle, the same data with Fig. 3B), or 6.0 solutions (blue square). Shown are mean \pm S.E. ($n = 4$ to 6). The lines were drawn by fitting to the Hill equation (pH

5.0: red line, pH 5.5: black line, pH 6.0: blue line).

Table 1. Compositions of solutions (mM). pH was adjusted with CsOH or NMDG.

	NMDG	CsOH	Glutamate	HCl	HEPES	MES	EGTA	CaCl ₂	MgCl ₂	pH
Pipette solution		86- 100			200		10		2	7.3
NMDG-Glutamate-rich solution pH 7.4	155-157		150		10			2		7.4
NMDG-Glutamate-rich solution pH 6.0	151-152		150			10		2		6.0
NMDG-Glutamate rich solution pH 5.5	149-150		155			10		2		5.5
NMDG-Glutamate rich solution pH 5.0	139-140		160			10		2		5.0
NMDG-Chloride rich solution pH 7.4	156-159			150	10			2		7.4
NMDG-Chloride rich solution pH 6.0	158			150		10		2		6.0
NMDG-Chloride rich solution pH 5.5	153-154			150		10		2		5.5
NMDG-Chloride rich solution pH 5.0	151			150		10		2		5.0

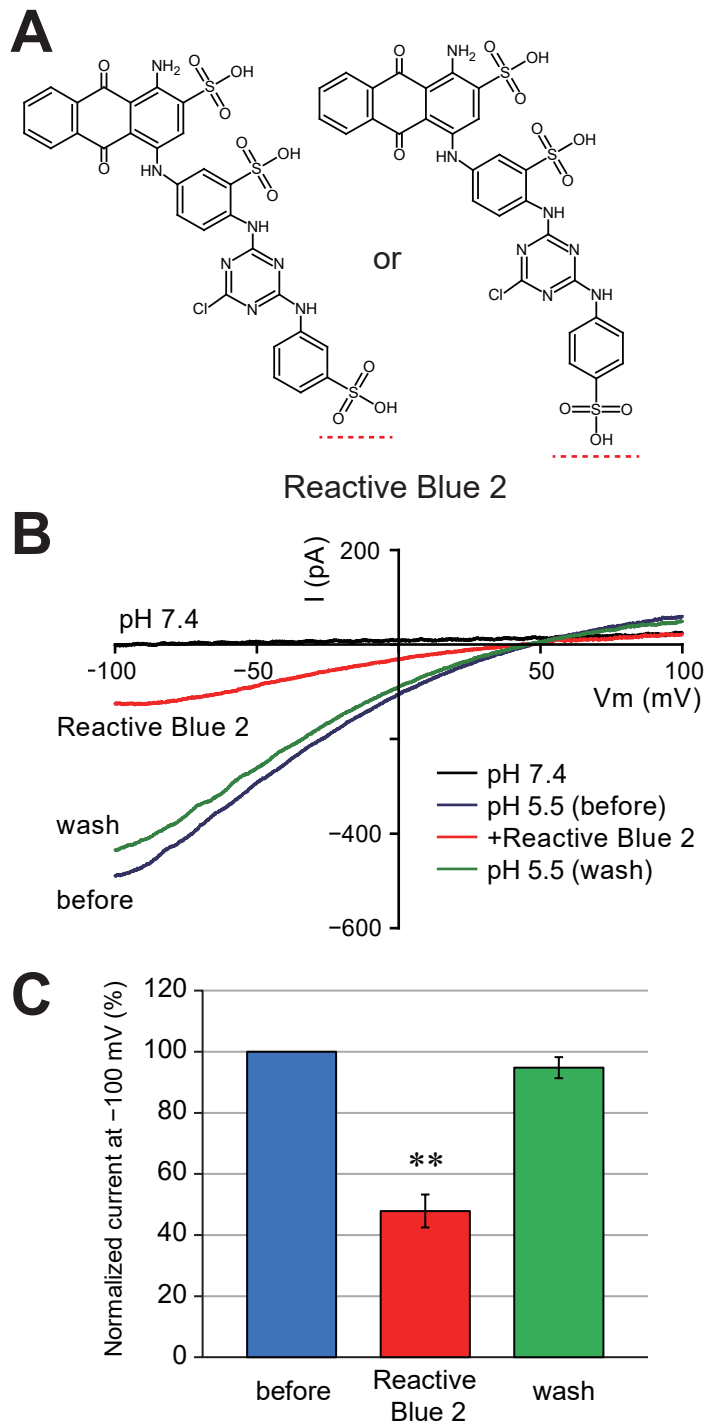
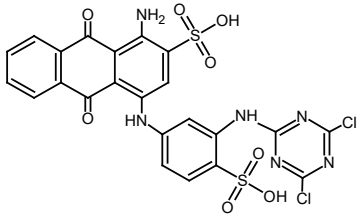
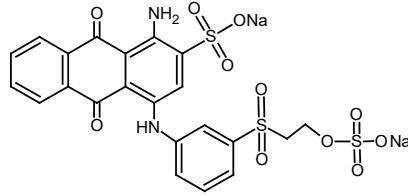


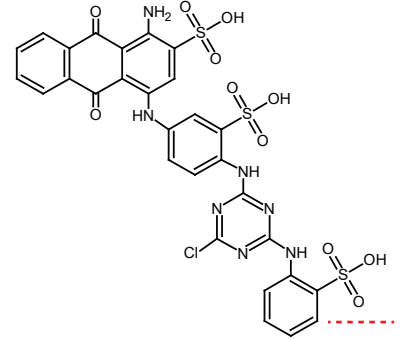
Fig. 1. Islam *et al.*

A

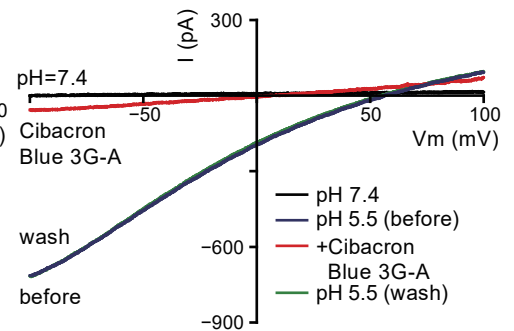
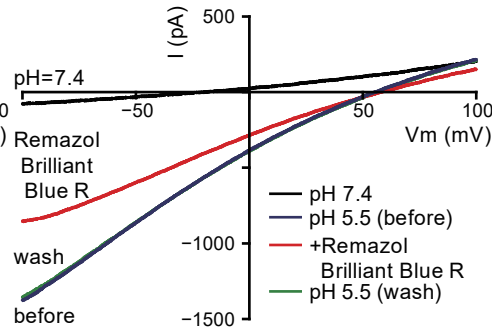
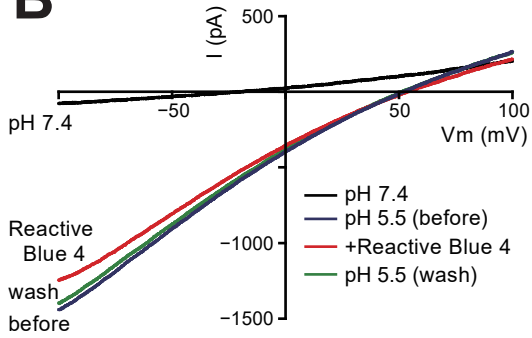
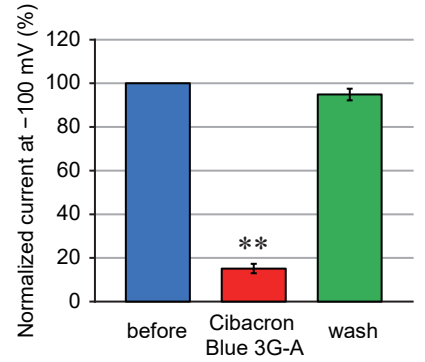
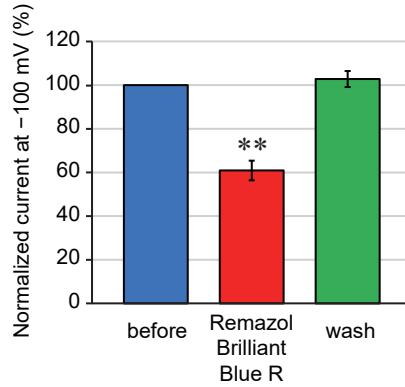
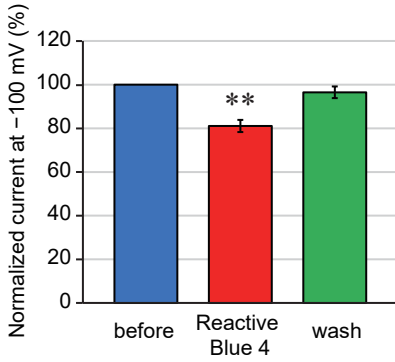
Reactive Blue 4



Remazol Brilliant Blue R Salt



Cibacron Blue 3G-A

B**C**Fig. 2. Islam *et al.*

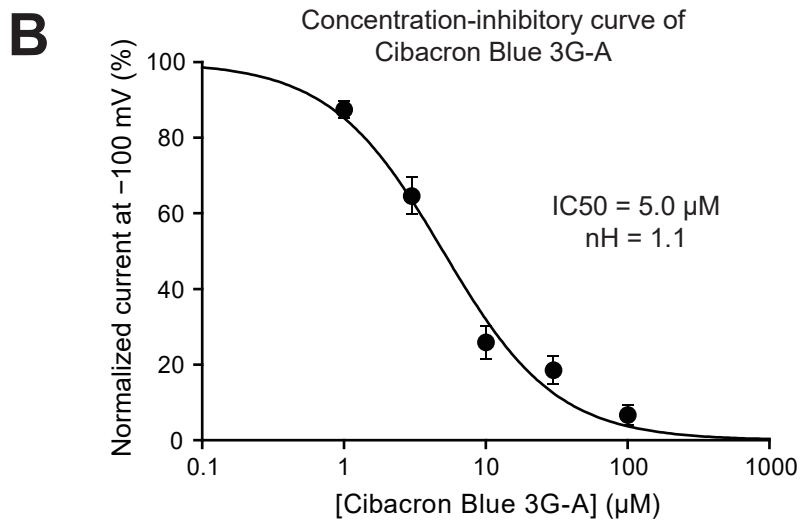
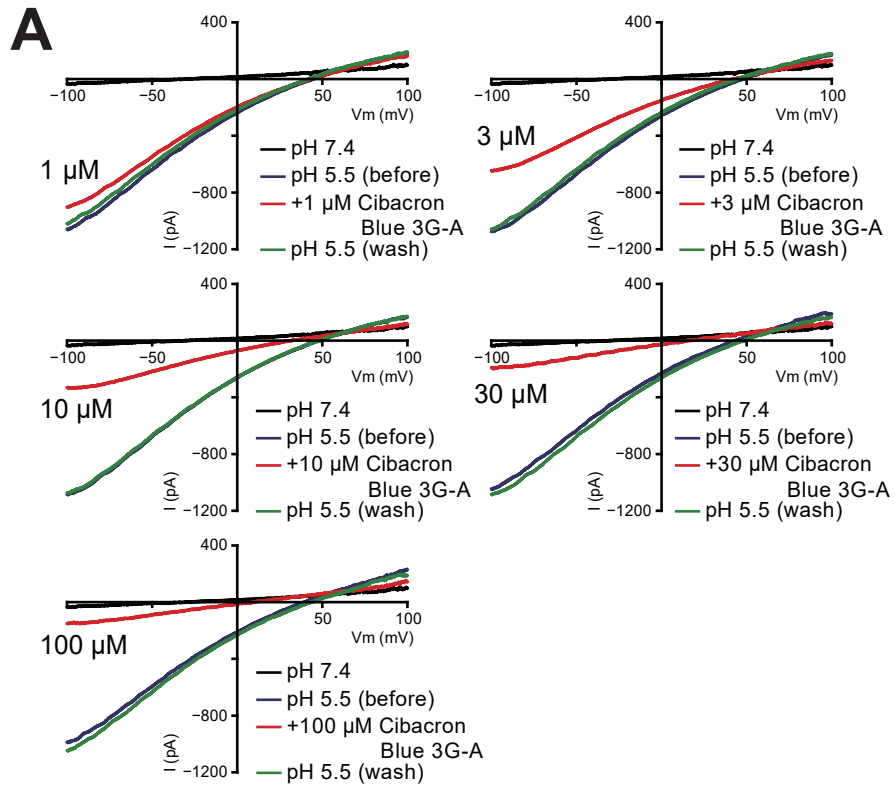


Fig. 3. Islam *et al.*

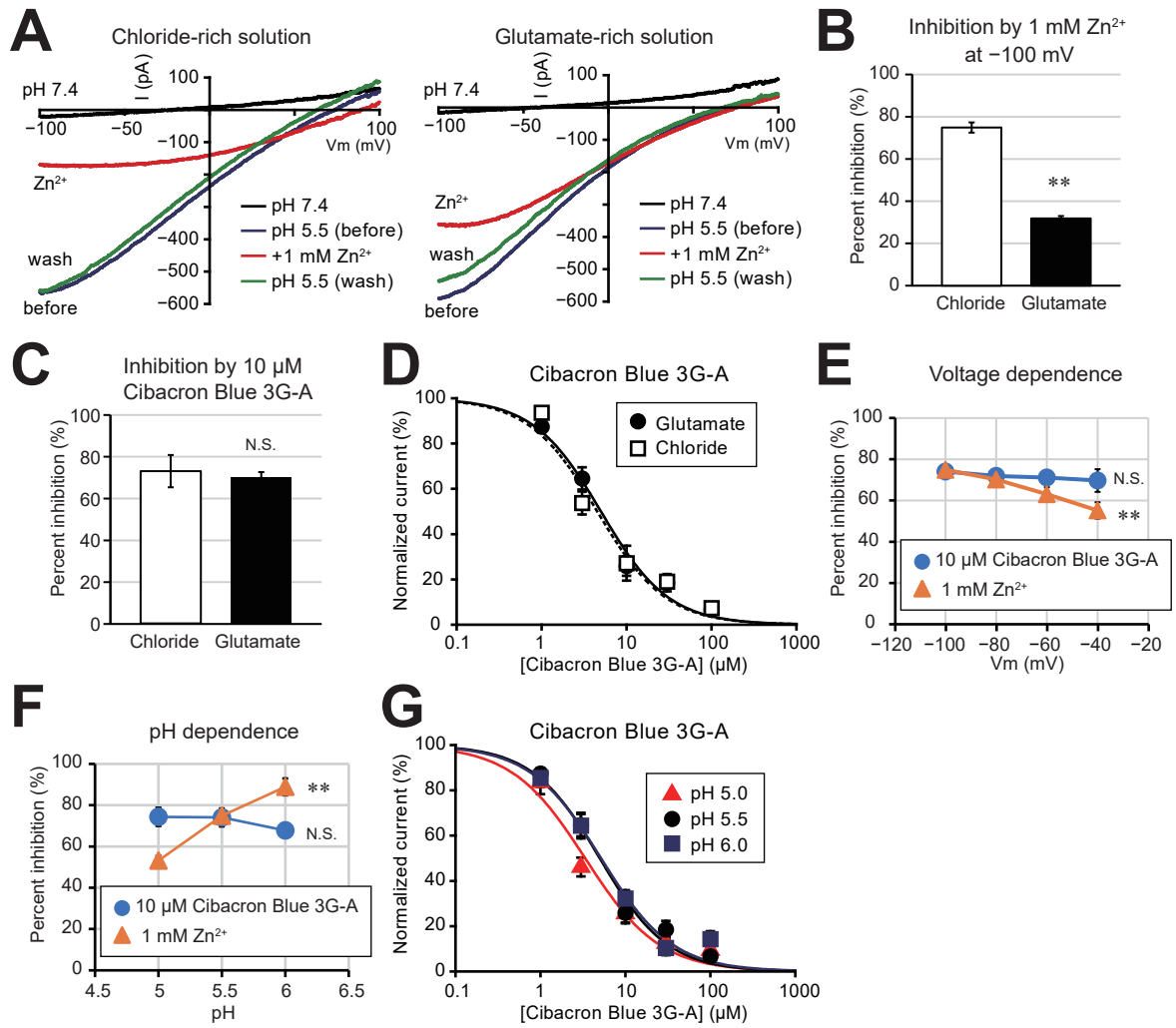


Fig. 4. Islam *et al.*